JVI Journals.ASM.org

Drosophila melanogaster as a Model Organism for Bluetongue Virus Replication and Tropism

Andrew E. Shaw,[a] Eva Veronesi,[b] Guillemette Maurin,[c] Najate Ftaich,[c] Francois Guiguen,[c] Frazer Rixon,[a] Maxime Ratinier,[a] Peter Mertens,[b] Simon Carpenter,[b] Massimo Palmarini,[a] Christophe Terzian,[c] and Frederick Arnaud[c]

MRC-University of Glasgow Centre for Virus Research, Institute of Infection, Immunity and Inflammation, College of Medical and Veterinary Life Sciences, University of Glasgow, Glasgow, United Kingdom[a]; Institute for Animal Health, Vector-borne Viral Diseases Programme, Pirbright, Surrey, United Kingdom[b]; and UMR754, INRA, Université Claude Bernard, Ecole Pratique des Hautes Etudes, Université de Lyon, SFR BioSciences Gerland-Lyon Sud, Lyon, France[c]

Bluetongue virus (BTV) is the etiological agent of bluetongue (BT), a hemorrhagic disease of ruminants that can cause high levels of morbidity and mortality. BTV is an arbovirus transmitted between its ruminant hosts by *Culicoides* biting midges (Diptera: Ceratopogonidae). Recently, Europe has experienced some of the largest BT outbreaks ever recorded, including areas with no known history of the disease, leading to unprecedented economic and animal welfare issues. The current lack of genomic resources and genetic tools for *Culicoides* restricts any detailed study of the mechanisms involved in the virus-insect interactions. In contrast, the genome of the fruit fly (*Drosophila melanogaster*) has been successfully sequenced, and it is used extensively as a model of molecular pathways due to the existence of powerful genetic technology. In this study, *D. melanogaster* is investigated as a model for the replication and tropism of BTV. Using reverse genetics, a modified BTV-1 that expresses the fluorescent mCherry protein fused to the viral nonstructural protein NS3 (BTV-1/NS3mCherry) was generated. We demonstrate that BTV-1/NS3mCherry is not only replication competent as it retains many characteristics of the wild-type virus but also replicates efficiently in *D. melanogaster* after removal of the bacterial endosymbiont *Wolbachia pipientis* by antibiotic treatment. Furthermore, confocal microscopy shows that the tissue tropism of BTV-1/NS3mCherry in *D. melanogaster* resembles that described previously for BTV in *Culicoides*. Overall, the data presented in this study demonstrate the feasibility of using *D. melanogaster* as a genetic model to investigate BTV-insect interactions that cannot be otherwise addressed in vector species.

Bluetongue virus (BTV) is an arbovirus belonging to the genus *Orbivirus* (family *Reoviridae*) that is biologically transmitted between its ruminants hosts by vector species of *Culicoides* biting midge (Diptera: Ceratopogonidae). In susceptible hosts, infection with BTV can lead to bluetongue (BT), a hemorrhagic disease of major importance for international trade and animal welfare (67). Historically, BTV has made only occasional incursions into Europe (46, 48, 73). Since 1998, however, BTV outbreaks have occurred virtually every year, resulting in severe economic losses across a wide geographic region (3, 45, 49, 78). Although severe clinical disease has been primarily restricted to improved wool and mutton breeds of sheep, the BTV-8 serotype, which entered Northern Europe in 2006 (15, 71), recorded relatively high case fatality rates in cattle (up to 1%) and a range of severe clinical signs (19, 50, 74, 78).

BTV is a complex nonenveloped virus with a 10-segmented double-stranded RNA (dsRNA) genome that encodes 7 structural proteins (VP1 to VP7) and 4 distinct nonstructural proteins (NS1, NS2, NS3/NS3A, and NS4) (5, 51, 60, 62). The virus particle is organized into three icosahedral protein capsids with an outer shell formed by VP2 and VP5, an inner capsid (or "outer core") composed of VP7, and an innermost layer (or "subcore") formed by VP3 (31, 32). The subcore surrounds the viral transcription complexes, composed of VP1 (polymerase), VP4 (capping enzyme), and VP6 (helicase) proteins, and the viral genomic segments (31, 61). The function of NS1 has yet to be fully defined, although it has been associated with cytopathogenesis (57) and the formation of characteristic tubules within the cytoplasm of infected cells (52). NS2 plays a key role in the formation of viral inclusion bodies (VIBs), where the assembly of new viral progeny takes place (11, 70). NS3/NS3A facilitates viral release, either by increasing plasma membrane permeability or by viral budding, according to the host cell considered (34, 39). NS4, the most recently described nonstructural protein of BTV, favors BTV replication in cells pretreated with interferon (5, 60).

Culicoides imicola is regarded as the major vector species in Africa (21) and Southern Europe (8, 48). It has been speculated that the progressive spread of this species in Europe is due to global warming and, in turn, is responsible for the increasing emergence of BTV in naïve European livestock (59). However, the recent BTV-8 outbreak in Northern Europe occurred beyond the northernmost limit of *C. imicola* (47), confirming earlier studies that had implicated Palearctic *Culicoides* species in the transmission of this virus (15). This hypothesis was later confirmed by the isolation of BTV from field-collected specimens that belong to the *Culicoides obsoletus* and *Culicoides pulicaris* groups, which are abundant in Central and Northern Europe (13, 20, 66), and the successful infections of both groups in the laboratory (14). In light of this evidence, the whole of Europe is currently regarded as "at risk" for the emergence of bluetongue and other arthropod-borne diseases (33, 44, 58).

Studies of *Culicoides*-orbivirus interactions have been hampered by the inability to successfully colonize the major BTV vec-

Received 17 January 2012 **Accepted** 30 May 2012
Published ahead of print 6 June 2012
Address correspondence to Frederick Arnaud, Frederick.Arnaud@univ-lyon1.fr.
A.E.S. and E.V. contributed equally to this article.

doi:10.1128/JVI.00131-12

tor species of Africa and Europe. Current understanding of the process of BTV infection and dissemination within the insect hosts are based almost entirely upon a single colonized species, *Culicoides sonorensis* (44). These studies have indicated that vector competence for BTV is determined in part by the presence of natural barriers to virus dissemination within adult *Culicoides* organisms. These barriers include (i) a mesenteron infection barrier (MIB) that controls the initial establishment of persistent gut infections upon BTV ingestion, (ii) a mesenteron escape barrier (MEB) that sequestrates BTV in gut cells, and (iii) a dissemination barrier (DB) that prevents infection of secondary organs, including salivary glands (24–26, 40, 46). Intrathoracic inoculation of adult *Culicoides* with BTV, however, leads to full dissemination of the virus and infection of secondary organs as a result of bypassing these barriers (9, 25, 40).

The lack of an accurately sequenced and annotated *Culicoides* genome and, consequently, the absence of genetic tools available for these organisms have restricted studies of *Culicoides*-orbivirus interactions. To date, the fruit fly (*Drosophila melanogaster*) genome is better characterized and understood than any other insect species, and it has been used in a vast array of studies of development and microbial pathogenesis, illustrating pathway conservation among vertebrates and invertebrates (17, 64, 72). Moreover, many of the classical signal transduction systems, including those involved in the immune response, were first identified in *D. melanogaster* using forward genetic screens (22, 43). More recently, it has become increasingly common to use *D. melanogaster* to study insect-pathogen interactions (17, 65). For instance, the bacterial endosymbiont *Wolbachia pipientis* (*w*Mel strain) of *D. melanogaster* increases resistance to infection by several RNA viruses, including many mosquito-transmitted arboviruses that are pathogenic in humans (6, 30, 36, 53, 69).

In this study, reverse genetics was used to generate a modified strain of BTV-1 expressing the mCherry fluorescent protein fused to NS3/NS3A (BTV-1/NS3mCherry). We demonstrate that BTV-1/NS3mCherry is able to replicate *in vitro* as well as *in vivo* in *C. sonorensis*, a competent vector for BTV. Furthermore, this virus was found to replicate efficiently *in vivo* in *D. melanogaster* after removal of *W. pipientis* infections by treatment with tetracycline. Finally, confocal analysis revealed that, similar to what has been observed in its insect vector (26), BTV replicates in the fat bodies, salivary glands, and proventriculi (foregut-midgut junction) of infected *D. melanogaster* flies.

MATERIALS AND METHODS

Cells. BSR cells (a clone of BHK-21) were kindly provided by Karl K. Conzelmann and were maintained in Dulbecco's modified Eagle's medium (DMEM) supplemented with 5% fetal bovine serum (FBS) and 25 μg/ml penicillin/streptomycin (P/S). Bovine fetal aorta endothelial (BFAE) cells were grown in Ham's F12 medium supplemented with 20% FBS and P/S. Both cell lines were incubated at 35 to 37°C in 5% CO_2. The KC cells used were originally derived from *C. sonorensis* embryos and were grown in Schneider's medium supplemented with 15% FBS and 25 μg/ml P/S at 25°C (77).

Plasmids and cloning. The 10 plasmids required to rescue the BTV-1 strain have been described previously (60). Each plasmid contains a single BTV genomic segment flanked by an N-terminal T7 promoter and a C-terminal restriction site to allow linearization and *in vitro* transcription of viral-like capped RNA. pUCBTV-1_Seg-10XhoI/EcoRVmod contains BTV-1 Seg-10 and was produced by site-directed mutagenesis inserting XhoI and EcoRV restriction sites into the region between the two predicted transmembrane domains of the NS3/NS3A protein (2). The mCherry coding sequence was amplified by PCR from pCMVRab5 WT-Cherry plasmid (55) using PfuUltra II Fusion HS DNA polymerase (Agilent). The PCR product was subsequently digested with XhoI and EcoRV and ligated into pUCBTV-1_Seg-10XhoI/EcoRVmod in order to obtain pBTV-1_Seg-10_mCherry. Detailed descriptions of primers and cloning procedures are available upon request.

BTV rescue. The wild-type (wt) BTV-1 and BTV-1/NS3mCherry were rescued by reverse genetics as already described (10, 60). Briefly, the rescue plasmids were digested with SapI or BsaI to generate exact 3′ termini of authentic BTV segments and were then used as the templates for *in vitro* transcription of BTV-like capped RNA. To rescue BTV, BSR cells were initially transfected with 1×10^{11} RNA copies of each segment encoding VP1, VP3, VP4, NS1, NS2, and VP6. After 18 h, the cells were further transfected with all 10 BTV segments, including the modified segment 10 encoding NS3mCherry. Transfection assays were performed using Lipofectamine 2000 (Invitrogen). Three hours after the second transfection, the medium was replaced with an agar overlay and cells were incubated at 35°C until plaques appeared. Individual plaques were then picked through the overlay, resuspended in 500 μl of DMEM, and used to infect BSR cells. Once the cytopathic effect (CPE) was advanced, the supernatant was separated from the cellular debris and stored as aliquots at 4°C. The cellular debris was resuspended in 1 ml TRIzol (Invitrogen), and the RNA was extracted according to the manufacturer's instructions. The dsRNA and single-stranded RNA (ssRNA) fractions were separated by precipitating the total RNA in the presence of 2 M lithium chloride.

The genome profiles of wt BTV-1 and BTV-1/NS3mCherry were analyzed by 1% agarose gel electrophoresis (AGE). Rescue assays were also performed and stained with crystal violet to assess the efficiency of virus rescue.

Confocal and electron microscopy. The day before infection, 1×10^5 BSR cells were plated in two-well glass chamber slides (LabTek) in 1 ml of growth medium. Subsequently, cells were infected with wt BTV-1 or BTV-1/NS3mCherry at a multiplicity of infection (MOI) of 0.001 by replacing the growth medium with 1 ml of virus diluted in DMEM (without serum) and incubated at 37°C for 24 h. The cells were then processed as already described (1, 54). Virus replication was detected using rabbit polyclonal anti-NS3 (for wt BTV-1) or anti-NS2 (for BTV-1/NS3mCherry) antibody. Goat anti-rabbit IgG conjugated to Alexa Fluor 488 (Molecular Probes) was used as a secondary antibody. Slides were mounted with medium containing DAPI (4′,6-diamidino-2-phenylindole; Vectashield, Vector Laboratories) and analyzed with a Leica TCS SP2 confocal microscope.

For electron microscopy, BSR cells were plated in 3.5-cm-diameter dishes and infected at an MOI of 0.05 for 2 h at 37°C. At 24 h postinfection (p.i.), the cells were fixed for 1 h at 4°C with 2.5% gluteraldehyde and 1% osmium tetroxide and subsequently pelleted through 1% SeaPlaque agarose (Flowgen). Cells were embedded in Epon 812 resin, dehydrated in a graded alcohol series, and then "cut" and analyzed in a Joel 1200 EX II electron microscope.

Virus growth curves. BSR or BFAE cells (2×10^5) were plated in 12-well plates 1 day prior to infection. The cells were subsequently infected at an MOI of 0.05 for 2 h with the appropriate virus dilution in DMEM. KC cells (2×10^6) were plated in 12-well plates 1 day prior to infection. The cells were subsequently infected at an MOI of 0.005 for 2 h with the appropriate virus dilution in Schneider's medium. The inocula were then discarded, cells were washed with DMEM, and 1 ml of growth medium was added. Mammalian cells were then incubated at 37°C and KC cells at 28°C. At 0, 8, 24, 48, and 72 h p.i., 100 μl of supernatant was removed and replaced with 100 μl of fresh growth medium. The supernatant samples were clarified by centrifugation at $500 \times g$ for 5 min, and the cell-free fractions were titrated by limiting dilution assays in BSR cells as described previously (12, 60).

To determine the relative level of intracellular versus extracellular virus, 1×10^5 BSR or BFAE cells were first plated in 24-well plates. The next

day, the cells in multiple wells were infected at an MOI of 0.05 for 2 h. The inocula were discarded, the cells were washed, and 0.5 ml of complete medium was added. At 24 h p.i., before the appearance of CPE, the supernatant was harvested from two wells and stored at 4°C. The cell sheets were disrupted by freeze-thawing, and the cellular material was resuspended in 0.5 ml of DMEM. The supernatant and cellular fractions were clarified by centrifugation, and the supernatants were titrated by a limiting dilution assay. Each experiment was repeated four times. The ratios between intracellular and extracellular viral titers were calculated, and statistical analyses were performed with a Wilcoxon nonparametric test to compare two median percentages using R software (Comprehensive R Archive Network; http://www.R-project.org).

Western blotting. BSR cells were plated in 12-well plates and infected at an MOI of 0.01. After 24 h, the cells were harvested in 100 μl of sample buffer. Proteins were separated by SDS-PAGE, transferred to Amersham Hybond-P (polyvinylidene difluoride [PVDF]) membranes (GE Healthcare), and incubated for 1 h at room temperature with polyclonal rabbit antibodies against BTV NS1, BTV NS3, or a monoclonal mouse antibody against gamma tubulin (Sigma-Aldrich) as appropriate (60). Subsequently, the membranes were incubated for 1 h at room temperature in the presence of a horseradish peroxidase-conjugated secondary antibody (GE Healthcare). Finally, the membranes were washed and developed with ECL Plus (GE Healthcare), followed by exposure to X-ray film (GE Healthcare).

***Culicoides* infection assays.** *Culicoides sonorensis* adults were produced from the colony maintained at the Pirbright laboratory (7). Two- to 3-day-old females ($n = 60$) were intrathoracically injected with 0.2 μl of BTV-1/NS3mCherry (1.2×10^5 PFU/ml), wt BTV-1 (1×10^6PFU/ml) as a positive control, or Schneider's medium as a negative control and then incubated at 25°C in a netted waxed pillbox (Watkins and Doncaster, Stainton, United Kingdom) with a wet cotton pad on the top of it (5% sucrose solution) that was provided daily as a food source. At day 10 p.i., surviving females were collected for analysis. Each specimen was individually homogenized in a final volume of 1 ml of Schneider's medium supplemented with 1% P/S and 1% amphotericin B using a Qiagen TissueLyser as described previously (75). Homogenates from day 10 p.i. were individually titrated by limiting dilution assays in BSR cells (12, 60).

***D. melanogaster* and *Wolbachia*.** The wild-type Canton-S strain and the transgenic *D. melanogaster* strain (w; P{w+, GAL4-YP1.JMR}20) (here referred to as Yolk-Gal4) were maintained at 23°C on axenic medium. The P{GAL4-YP1.JMR} transgene can specifically direct expression of the yeast GAL4 transcription factor in the fat body cells of adult *D. melanogaster* females (28). The presence of *W. pipientis* in the *D. melanogaster* strains was assessed by PCR on DNA extracted from 10 individual *D. melanogaster* flies. Briefly, *D. melanogaster* flies were frozen at −20°C for at least 20 min and subsequently homogenized in 50 μl homogenization buffer (10 mM Tris-HCl [pH 8.2], 1 mM EDTA, 25 mM NaCl, and 200 μg/ml proteinase K). After 30 min of incubation at 37°C, proteinase K was inactivated by heating the samples for 10 min at 95°C. Cell debris was pelleted by centrifugation, and the resulting supernatant was stored at 4°C until assayed by PCR. 99F/994R and wsp81/wsp691 were used as primers to amplify 16S rRNA genes and *wsp*, respectively, from several strains of *W. pipientis* as described previously (80). The mitochondrial 12S rRNA gene was amplified with primer pair 12SAI/12SBI as described elsewhere (56). The presence of closely related *w*Mel strains (*w*Mel or *w*MelPop) was confirmed by sequencing PCR products. A Yolk-Gal4 *W. pipientis*-free line was generated by adding 0.25 mg/ml of tetracycline to the medium (38). After two generations of tetracycline treatment, *D. melanogaster* flies were grown for at least four generations on normal media in order for them to recover before being used for experiments. The Canton-S strain treated with tetracycline was kindly provided by the laboratory of Jean-Luc Imler. The absence of *W. pipientis* was assessed in individual *D. melanogaster* flies ($n = 10$) using PCR as described above.

***D. melanogaster* infection.** Two- to 3-day-old Yolk-Gal4 females, treated or not treated with tetracycline, were intrathoracically injected with 0.345 μl of BTV-1/NS3mCherry virus (4.5 $\log_{10}$ 50% tissue culture infective dose [$TCID_{50}$]/ml) or supernatant from uninfected BSR cells (referred to as mock infected). After injection, 5 *D. melanogaster* flies were either collected immediately (day 0) or incubated at 28°C for 10 days (day 10) before collecting and processing. Day 0 and day 10 *D. melanogaster* flies were individually homogenized in a final volume of 1 ml Schneider's medium containing 10% fetal bovine serum, 2.5 μg/ml amphotericin B, 100 units/ml nystatin, 50 μg/ml gentamicin, and 25 μg/ml P/S. The homogenate debris was pelleted by centrifugation, and the supernatant was retained for subsequent fluorescence-activated cell sorter (FACS) analysis. Each experiment was repeated three times, and 40 to 60 individuals were injected during each experiment.

In addition, 2- to 3-day-old *Wolbachia*-free Canton-S and Yolk-Gal4 females ($n = 60$) were intrathoracically injected with 0.345 μl of wt BTV-1 or BTV-1/NS3mCherry virus at the same viral titer (2×10^4 PFU/ml) or mock infected with supernatant from uninfected BSR cells. At day 0 and day 10 p.i., 10 females were collected and individually homogenized in a final volume of 1 ml DMEM containing 10% fetal bovine serum, 2.5 μg/ml amphotericin B, 100 units/ml nystatin, 50 μg/ml gentamicin, and 25 μg/ml P/S. Homogenates were then individually titrated by limiting dilution assays in BSR cells (12, 60).

FACS analysis. In order to detect BTV-1/NS3mCherry-positive cells, FACS analysis was performed on KC cells (1.5×10^5 cells/well) inoculated with 100 μl of individual *D. melanogaster* homogenate in 96-well plates. Experiments were repeated three times. The cells were incubated for 5 days at 28°C and then resuspended in 1% paraformaldehyde (PFA) prior to FACS analysis. Five days postinoculation of KC cells was optimal for discrimination between the homogenates of *D. melanogaster* flies collected at day 0 and day 10 postinfection.

Titrations by endpoint dilution in KC cells (1.5×10^5 cells/well) were also performed for the *D. melanogaster* homogenates producing the greatest number of mCherry-positive cells by FACS analysis. Briefly, a 10-fold dilution series of each homogenate was added to a 96-well plate (100 μl/well using four replicates per dilution). Plates were sealed and incubated at 28°C. At 7 days postinoculation, each well was analyzed by FACS and scored as positive if >0.5% of cells were mCherry positive (with 0.5% being the upper limit of the background obtained with mock-infected *D. melanogaster* homogenates). The virus titers were calculated as a 50% endpoint and expressed as $\log_{10}$ $TCID_{50}$/ml, calculated using the Spearman-Karber formula (23). FACS analyses were performed with a BD LSR II cytometer using BD FACSDiva 6.1.2 software. Forward scatter (FSC-A) and side scatter (SSC-A) data were used to characterize events corresponding to the viable KC cells. Statistical analyses were also performed with a Wilcoxon nonparametric test to compare two median percentages using R software.

Imaging of BTV-infected *D. melanogaster* flies. Mock- and BTV-injected tetracycline-treated *D. melanogaster* flies (Yolk-Gal4) were collected at day 10 p.i. and incubated in 2% PFA at 4°C for 24 h. *D. melanogaster* flies were rinsed in phosphate-buffered saline (PBS) and incubated in 20% sucrose solution overnight at 4°C before being frozen at −80°C in cryo-embedding media (OCT). Whole-fly cryosections (20-μm thick) were prepared and laid on SuperFrost Ultra Plus glass slides (Dutscher). Slides were subsequently mounted using a Vectashield mounting medium containing DAPI and analyzed by confocal microscopy using a Leica TCS SP5 microscope.

RESULTS

Rescue of BTV-1/NS3mCherry. By reverse genetics, we have designed and rescued a BTV-1-based virus expressing the mCherry fluorescent protein, located between the two predicted transmembrane domains of NS3/NS3A (Fig. 1A and B). This virus (identified as BTV-1/NS3mCherry) formed several plaques on BSR cell monolayers, although rescue efficiency was lower than that of wt BTV-1 (Fig. 1C). The genome segment migration patterns of wt BTV-1 and BTV-1/NS3mCherry were compared by 1% AGE. The

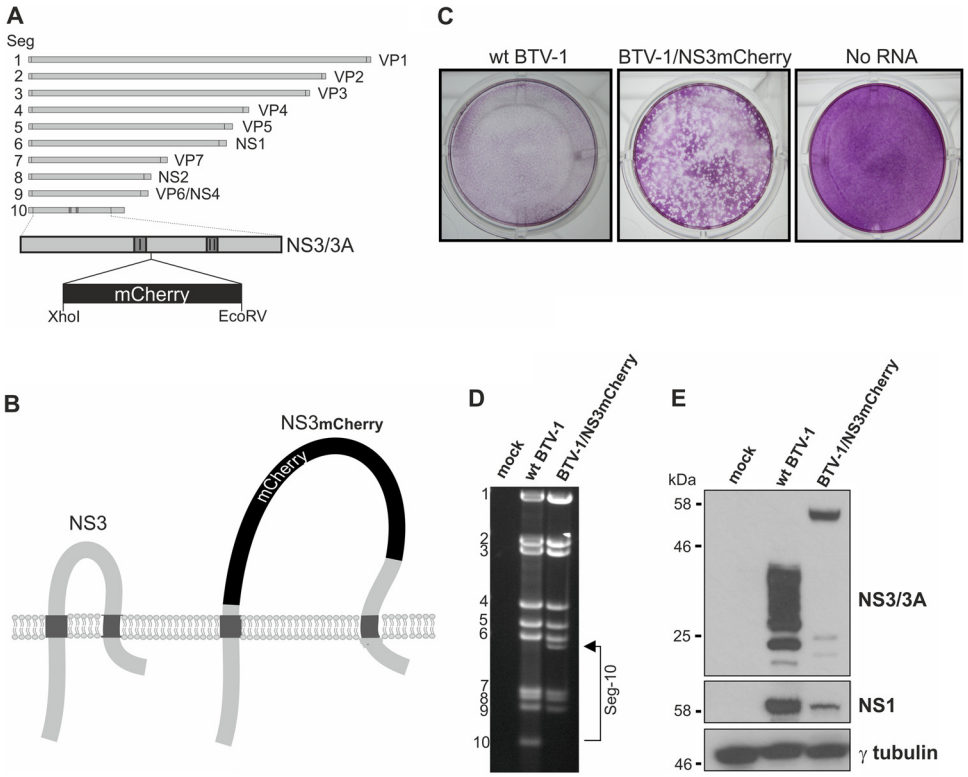

FIG 1 Rescue of a recombinant BTV-1 expressing the mCherry fluorescent protein. (A) XhoI and EcoRV sites were introduced into BTV-1 segment 10 (Seg-10) between the two transmembrane domains (I and II) of the NS3/3A protein. The restriction sites were then used to insert the mCherry fluorescent protein in frame with the NS3/NS3A coding sequence. (B) Based upon the predicted topology of the NS3 protein, mCherry is located in a loop on the noncytosolic side of the cell membrane (right), while leaving the cytosolic tails of the protein free to interact as per wild-type NS3 (left). (C) Crystal violet staining revealed that BTV-1/NS3mCherry was rescued efficiently from BSR cells. (D) wt BTV-1 and BTV-1/NS3mCherry display identical genomic profiles, except for Seg-10, which migrates at 822 and 1,530 nucleotides, respectively. (E) BSR cells were infected with wt BTV-1 or BTV-1/NS3mCherry, and lysates were analyzed by Western blotting with antibodies against viral NS1 and NS3/NS3A proteins. Note that, while the band corresponding to NS1 migrated at the same level for both wt BTV-1 and BTV-1/NS3mCherry, the band corresponding to NS3 migrated higher in BTV-1/NS3mCherry, due to the presence of the mCherry protein. Antibody against gamma tubulin was used as a loading control.

band corresponding to Seg-10 of BTV-1/NS3mCherry migrated more slowly than that of wt BTV-1, due to the presence of the mCherry coding sequence, confirming the incorporation of the modified Seg-10 into the BTV-1 genome (Fig. 1D). Protein bands were detected by Western blotting at 26 and 24 kDa (NS3 and NS3A, respectively), along with a smear at higher molecular weights typical of wt BTV-1 NS3/NS3A (Fig. 1E). In contrast, BTV-1/NS3mCherry displayed a band of approximately 53 kDa that corresponds to the NS3mCherry protein (Fig. 1E). NS1 was also detected in BSR cells infected with BTV-1/NS3mCherry, albeit at lower levels compared to wt BTV-1 NS1 (Fig. 1E).

Characterization of BTV-1/NS3mCherry. As mCherry is fused to NS3, a fluorescent signal is only observed when the recombinant virus enters the cell, replicates, and synthesizes its nonstructural proteins. By confocal microscopy, we observed mCherry expression in BSR cells infected with BTV-1/NS3mCherry. Moreover, the mCherry fluorescent signal was detected in the same cells as those expressing NS2 (Fig. 2A, panel ii), confirming that NS3mCherry is only expressed in cells with actively replicating BTVs. By electron microscopy, BSR cells infected with BTV-1/NS3mCherry displayed the hallmarks of BTV-infected cells, including the presence of NS1 tubules, VIBs containing progeny cores, and viral particles (Fig. 2B). Interestingly, viral particles budding at the plasma membrane were observed for wt BTV-1 but not BTV-1/NS3mCherry (Fig. 2B, panel iii).

Growth curves in BSR cells showed that BTV-1/NS3mCherry displays a slightly lower replication rate than wt BTV-1 (Fig. 3A). However, in BFAE and KC cells, wt BTV-1 replicated much more efficiently than BTV-1/NS3mCherry (Fig. 3B and C). In addition, the ratio between the intracellular and extracellular viral titers is significantly higher for BTV-1/NS3mCherry in BFAE cells (Wilcoxon sum of rank test, $P = 0.028$) than for BSR cells ($P > 0.05$), indicating a partial intracellular retention of the newly formed virion of BTV-1/NS3mCherry in this cell type compared to the wt BTV-1 (Fig. 3D and E). These data suggest that the function of NS3 on BTV egress (39) is partially compromised in the NS3mCherry fusion protein. Indeed, extensive passaging of BTV-1/NS3mCherry in BSR cells leads to the selection of deletion mutants that lack the intact mCherry reading frame (data not shown). However, BTV-1/NS3mCherry was able to replicate efficiently in injected *C. sonorensis* females (Fig. 3F).

wt BTV-1 and BTV-1/NS3mCherry replicate in *D. melanogaster*. Initial BTV-1/NS3mCherry infection assays in *D. melanogaster* were inconclusive, as the virus replicated only to low levels. We subsequently found that the Yolk-Gal4 *D. melanogaster* flies used for these experiments were positive for a strain of *W. pipientis*

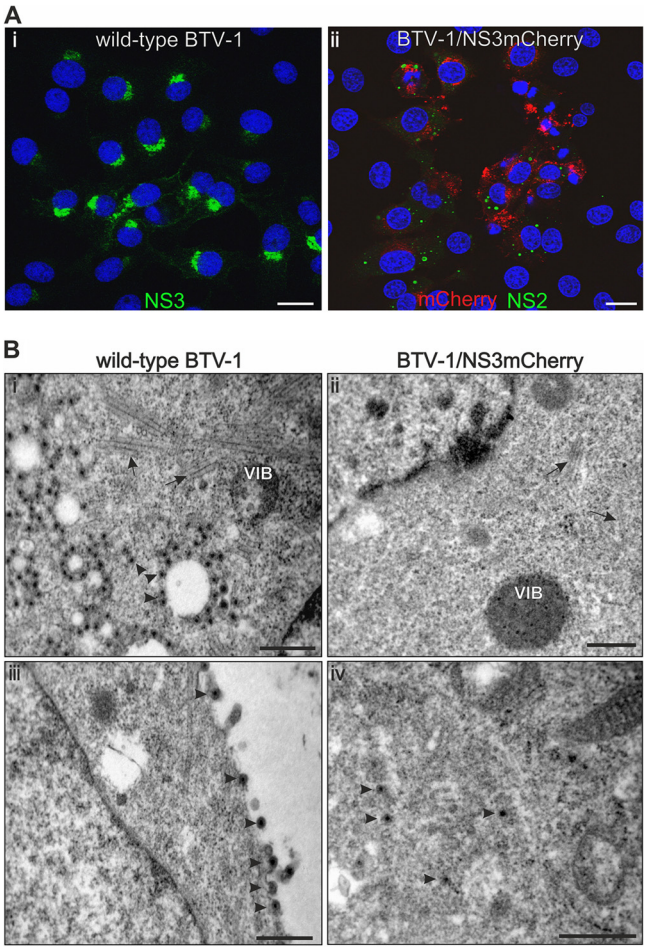

FIG 2 *In vitro* characterization of BTV-1/NS3mCherry. (A) Confocal microscopy of BSR cells infected with wild-type BTV-1 (i) or BTV-1/NS3mCherry (ii) at an MOI of 0.001 and fixed at 24 h p.i. Cells were immunolabeled using a polyclonal antiserum raised against NS3 (i) or NS2 (ii) and an Alexa Fluor 488 secondary antibody (shown in green) as described in Materials and Methods; BSR cells positive for BTV-1/NS3mCherry infection are shown in red (ii). NS2 immunolabeling indicates the presence of replicating viruses and was only observed in mCherry-expressing cells. Scale bars, 20 μm. (B) BSR cells infected with either wild-type BTV-1 (i and iii) or BTV-1/NS3mCherry (ii and iv) were fixed at 24 h p.i. and prepared for electron microscopy. Typical features associated with BTV-1 infection were observed, including viral inclusion bodies (VIB), NS1 tubules (arrows), and viral particles (arrowheads). Scale bars, 0.5 μm.

that is closely related to *w*Mel (Fig. 4A and data not shown) and known to increase the resistance to infection by several arboviruses (6, 30, 36, 53, 69). We therefore used tetracycline treatment to generate a *W. pipientis*-free line of *D. melanogaster* (Yolk-T) from the original, untreated Yolk-Gal4 stock (Yolk-NT). We were not able to detect *W. pipientis* by PCR in subsequent generations of *D. melanogaster* flies that had been treated with tetracycline, confirming the success of treatment (Fig. 4A). Yolk-Gal4 females, treated or not treated with tetracycline, were intrathoracically inoculated with BTV-1/NS3mCherry (or DMEM as a mock-infection control) and either collected immediately postinfection (D0) or incubated at 28°C for 10 days (D10) prior to collection (Fig. 4B). KC cells were infected with mock-infected or BTV-1/NS3mCherry-infected homogenates of day 0 and day 10 *D. melanogaster* flies and then incubated at 28°C for 5 days before analysis by FACS (Fig. 4B). KC cells inoculated with mock-infected homogenates displayed a background ranging from 0 to 0.4% of mCherry-positive cells at 5 days p.i. (regardless of whether or not the *D. melanogaster* flies had been treated with tetracycline) (Fig. 4C). Similarly, *D. melanogaster* injected with BTV-1/NS3mCherry and harvested immediately (day 0, input virus) yielded a low percentage (0.1 to 0.5%) of mCherry-positive cells, with a median value of 0.2% (Fig. 4C and D). KC cells infected with Yolk-NT homogenates from day 10 also displayed a low percentage of mCherry-positive cells, with a median value of 0.1%, indicating low levels of BTV replication (Fig. 4C and D). Together, these data reveal that Yolk-NT *D. melanogaster* failed to show any statistically significant BTV replication (as detected by mCherry signal) between day 0 and day 10 (Wilcoxon sum of rank test, $P = 0.156$) (Fig. 4D). In contrast, the Yolk-T strain consistently displayed high levels of BTV-1/NS3mCherry infection (36.2 to 62%), with a median value of 48.5% and a statistically significant increase in the levels of BTV replication between day 0 and day 10 ($P = 4 \times 10^{-6}$) (Fig. 4D). BTV titration assays by endpoint dilution in KC cells showed that the upper values in day 10 *D. melanogaster* homogenates is equivalent to 2.75 $\log_{10}$ $TCID_{50}$/ml for the Yolk-NT strain and 5.75 $\log_{10}$ $TCID_{50}$/ml for the Yolk-T strain (Fig. 4D).

Yolk-Gal4 is a transgenic strain that expresses a high quantity of the yeast transcription factor Gal4 in the fat body (28) and, therefore, may be less fit than other *D. melanogaster* strains. To this end, transgenic Yolk-T and wild-type Canton-S *Wolbachia*-free females (Fig. 4A) were intrathoracically inoculated with the same amount of wt BTV-1 or BTV-1/NS3mCherry at the same viral titer (2×10^4 PFU/ml) and either collected immediately postinfection or incubated at 28°C for 10 days prior to collection. Titration assays by endpoint dilution in BSR cells show a significant increase of the viral titers in day 10 Yolk-T and Canton-S *D. melanogaster* strains for both wt BTV-1 and BTV-1/NS3mCherry (Wilcoxon sum of rank tests, $P < 10^{-4}$ between day 0 and day 10 titers) (Fig. 4E and F). BTV-1/NS3mCherry replicated in injected *D. melanogaster* at a lower rate than wt BTV-1 ($P = 0.003$ in Yolk-T; $P = 0.005$ in Canton-S). Both wt BTV-1 and BTV-1/NS3mCherry displayed a lower replication rate in the Canton-S strain than in the Yolk-T *D. melanogaster* strain ($P = 0.009$ for wt BTV-1; $P = 0.036$ for BTV-1/NS3mCherry) (Fig. 4E and F).

BTV-1/NS3mCherry tropism. The fluorescence characteristics of BTV-1/NS3mCherry were used to identify tissues/organs in which BTV replication occurs in the *D. melanogaster* model. No mCherry signal was observed in mock-injected *D. melanogaster* (Fig. 5A to C), but an intense signal was detected in day 10 Yolk-T injected with BTV-1/NS3mCherry (Fig. 5D to O). The proventriculus (i.e., the junction between the foregut and midgut) was found to be heavily infected by BTV-1/NS3mCherry, with the fluorescent signal particularly restricted to the ectodermal cells of foregut origin (Fig. 5D to F). No signal was observed in the endodermal cells originating from the midgut (Fig. 5F). BTV-1/NS3mCherry replication was also observed in the salivary glands and fat body cells throughout *D. melanogaster*-infected individuals (Fig. 5G to O).

DISCUSSION

In this study, we demonstrate that *D. melanogaster* can be used as a highly malleable model for studies on BTV replication and tropism in insects. In addition, we developed a replication-compe-

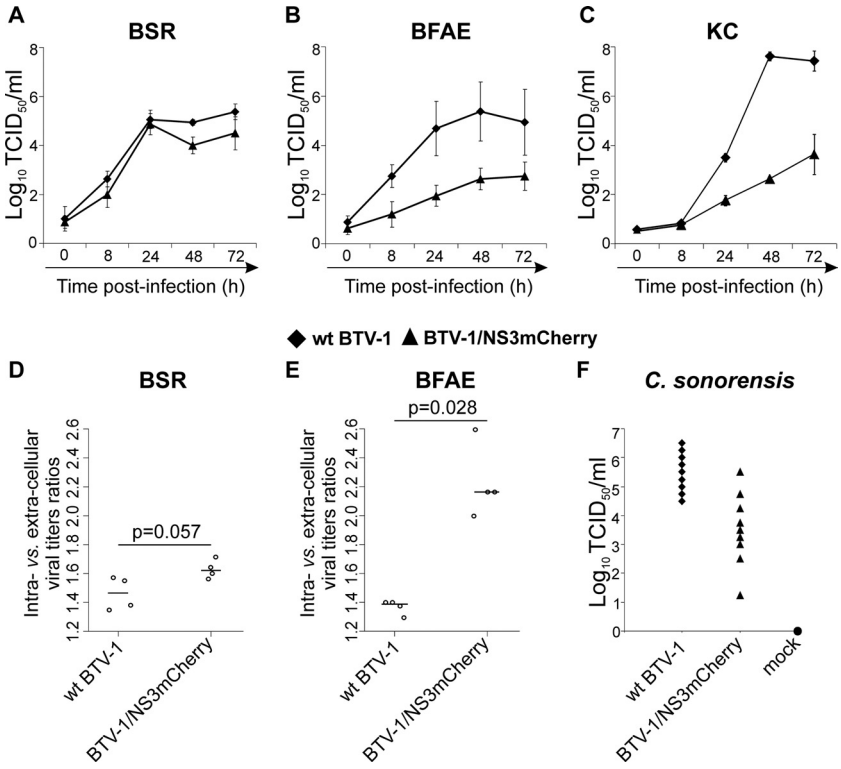

FIG 3 Replication rates of BTV-1/NS3mCherry. (A to C) *In vitro* virus growth curves were performed in BSR (A), BFAE (B), or KC (C) cells infected with wt BTV-1 or BTV-1/NS3mCherry. Multiple time points postinfection were generated by sampling and titrating cell supernatants. The BTV-1/NS3mCherry growth curve was more similar to that of wt BTV-1 in BSR cells than in BFAE or KC cells, where the increase in BTV-1/NS3mCherry titer was slower. (D to E) The graphs display the ratio between the intracellular versus extracellular virus titers in BSR (D) or BFAE (E) cells at 24 h p.i. BTV-1/NS3mCherry ratios are significantly higher than the wt BTV-1 in BFAE ($P < 0.05$) but not in BSR cells. (F) To determine whether BTV-1/NS3mCherry was able to replicate *in vivo*, *C. sonorensis* females were injected intrathoracically with BTV-1/NS3mCherry (or Schneider's medium as a negative control, referred to as "mock"). The wt BTV was used in this experiment as a positive control. After 10 days of incubation, *C. sonorensis* were individually homogenized and titrated by dilution assays on BSR cells. As indicated by the graph, BTV-1/NS3mCherry is able to replicate in *C. sonorensis*.

tent BTV expressing the mCherry fluorophore within the viral NS3 protein (BTV-1/NS3mCherry), which can be visualized by microscopy in a straightforward manner and will aid future research on vector competence in *Culicoides*. NS3 has been shown to be involved in a "late stage" of virus morphogenesis to orchestrate virus release and thus represents a good candidate for modification (16). Both the carboxy and amino termini of the NS3 protein have been shown to be important for virus-cell interactions (4); therefore, simply abutting a fluorescent protein to either terminus would reasonably be expected to disrupt one of these interactions. To overcome this issue, we inserted the mCherry protein in a site between the two predicted transmembrane domains of NS3/NS3A (2) and, by reverse genetics, we successfully rescued the modified BTV-1/NS3mCherry.

As expected, some differences between the NS3 expressed by the wild-type BTV-1 and the NS3mCherry expressed by BTV-1/NS3mCherry were observed. Both NS3 and NS3A proteins are encoded by the RNA Seg-10 and translated from two alternative ATG codons (63). By Western blotting, BTV-1/NS3mCherry displayed only one band of approximately 53 kDa, corresponding to NS3mCherry (Fig. 1E). NS3A expression is generally much lower than that of NS3 (79), most likely because both compete for the cell translation machinery. In addition, NS1 and NS3 protein levels appear lower in BTV-1/NS3mCherry than in wt BTV-1 (Fig. 1E), possibly due to the slightly different replication rates of these two viruses in BSR cells (Fig. 3A). It is therefore possible that the level of NS3AmCherry proteins is too low to be detected in our experiment. A few weak bands of a low molecular weight were also observed (Fig. 1E) and may represent degradation products. Moreover, the smearing of the wt BTV-1 NS3/NS3A, most likely associated with glycosylated forms of the protein (16, 79), was not observed (Fig. 1E), suggesting that glycosylation of NS3mCherry may be blocked. Indeed, the mCherry sequence is inserted close (6 amino acids) to the N-linked glycosylation site within NS3/NS3A. Based upon its role in viral egress, this alteration could affect NS3 function, which may in turn explain the difference observed in virus growth curves in BFAE and KC cells (Fig. 3B and C). Indeed, BFAE cells, like KC cells, failed to show CPE upon BTV infection, suggesting a mechanism of viral egress mainly by budding (60). Therefore, the differences in replication kinetics of wt BTV-1 and BTV-1/NS3mCherry *in vitro* (Fig. 3B and C) and *in vivo* (Fig. 4E and F) as well as the significant intracellular retention of newly formed BTV-1/NS3mCherry virions in BFAE cells (Fig. 3E) most likely represent a partial defect of NS3mCherry to mediate viral exit. Interestingly, the disruption or removal of glycans from proteins involved in cell exit has caused similar defects in virus release by other viruses, such as West Nile virus and Japanese encephalitis virus (35, 41). Nevertheless, BTV-1/NS3mCherry was shown to replicate *in vivo* in intrathoracically inoculated *C. sonorensis* and in

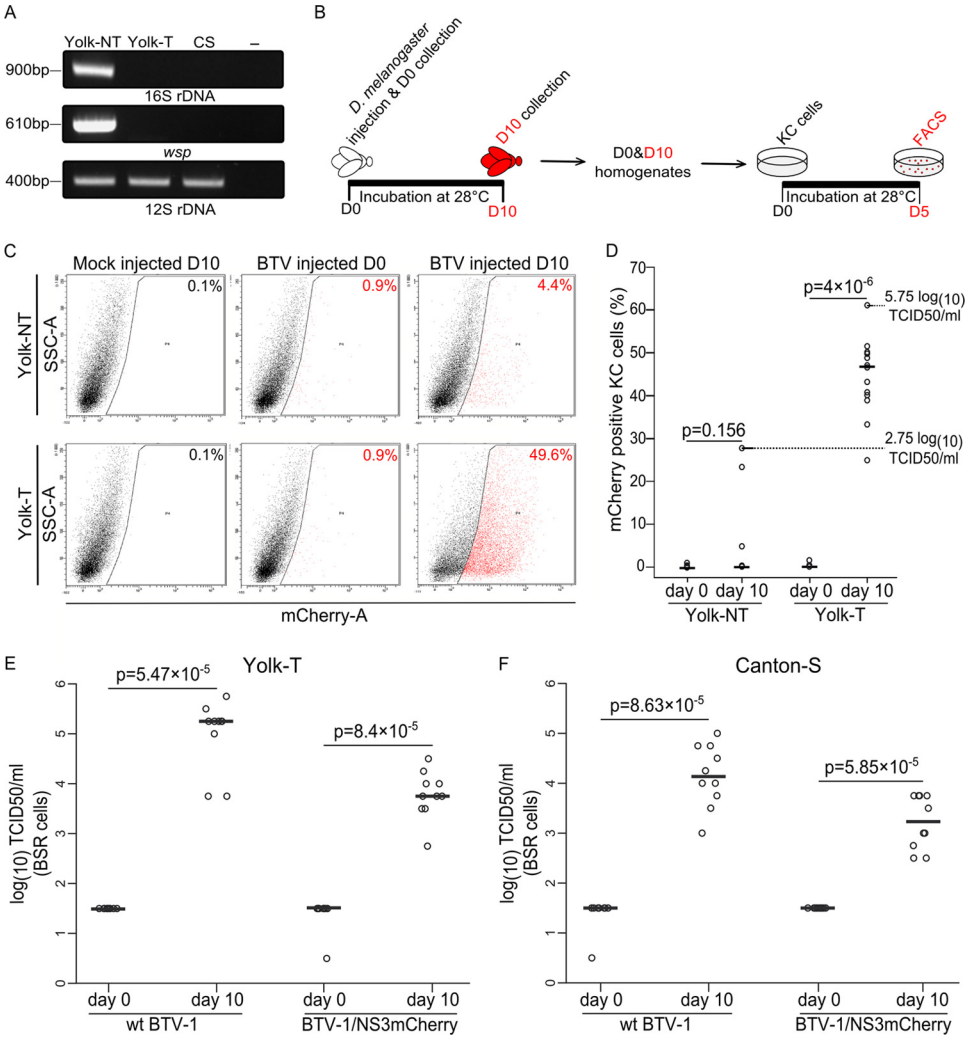

FIG 4 wt BTV-1 and BTV-1/NS3mCherry are able to replicate in *D. melanogaster*. (A) Specific PCR detection of *W. pipientis* before and after tetracycline treatment. Before tetracycline treatment, the Yolk-Gal4 strain (Yolk-NT) was found to be positive for *W. pipientis* using primers specific for 16S rRNA genes and *wsp*. In contrast, and as expected, the tetracycline-treated Yolk-Gal4 (Yolk-T) and Canton-S (CS) strains were found negative for *W. pipientis*. PCR amplification of mitochondrial 12S rRNA gene primers was used as a DNA extraction control. (B) Yolk-Gal4 *D. melanogaster* flies were injected with BTV-1/NS3mCherry and either harvested immediately (day 0, input virus) or incubated for 10 days prior to harvest (day 10). Each individual was homogenized and used to infect KC cells. Five days p.i., cells were analyzed by FACS. (C) Tetracycline-treated (Yolk-T) and untreated (Yolk-NT) *D. melanogaster* flies were injected with BTV-1/NS3mCherry (BTV) or virus-free medium (mock) and assayed as described above. *D. melanogaster* harvested immediately after injection (D0) showed very weak evidence of infection compared to those which had been mock injected (left versus middle panel). After 10 days of incubation (D10), the Yolk-T consistently showed high levels of infection, whereas the Yolk-NT showed only minimal evidence of viral replication (right panels). (D) The graph displays the percentage of mCherry-positive KC cells inoculated with *D. melanogaster* homogenates and harvested 5 days postinoculation. Horizontal bars represent the mean values of the data obtained from three independent experiments (5 individuals per day and per experiment). No significant difference was observed between day 0 and day 10 Yolk-NT homogenates ($P = 0.156$), whereas Yolk-T homogenates were highly permissive to BTV-1/NS3mCherry infection ($P = 4 \times 10^{-6}$). (E and F) Yolk-T (E) and Canton-S (F) *D. melanogaster* females were injected intrathoracically with wt BTV-1 or BTV-1/NS3mCherry at the same viral titer (2×10^4 PFU/ml) and either harvested immediately (day 0, input virus) or incubated for 10 days prior to collection (day 10). Each individual was homogenized and titrated by dilution assays on BSR cells. Horizontal bars represent the mean values of the data obtained (10 individuals per day and per experiment). All *P* values indicated between D0 and D10 titers are significant ($P < 10^{-4}$).

multiple cell lines, independent of any viral proteins provided in *trans*, while expressing a fluorescent form of NS3/NS3A.

The results reported in this study demonstrate that the wt BTV-1 and BTV-1/NS3mCherry replicate efficiently in both the transgenic Yolk-Gal4 and wild-type Canton-S *D. melanogaster* strains when introduced by intrathoracic inoculation. We noticed that BTV replication is significantly lower in Canton-S than in Yolk-Gal4. This difference may be explained by the fact that Yolk-Gal4 expresses a high quantity of the yeast transcription factor Gal4 in the fat body (28) and, therefore, may be less fit than wild-type Canton-S. Nonetheless, the Yolk-Gal4 strain may prove to be useful in future studies that require the specific knockdown of genes of interest in the fat bodies. During the course of the current study, evidence was also produced that *W. pipientis* can inhibit BTV replication in *D. melanogaster*. *Wolbachia* is a genus of bacteria that infects a high proportion of insect species, including *Drosophila* where it is widespread (18). It is recognized that certain species of *Wolbachia* are able to block infection by several patho-

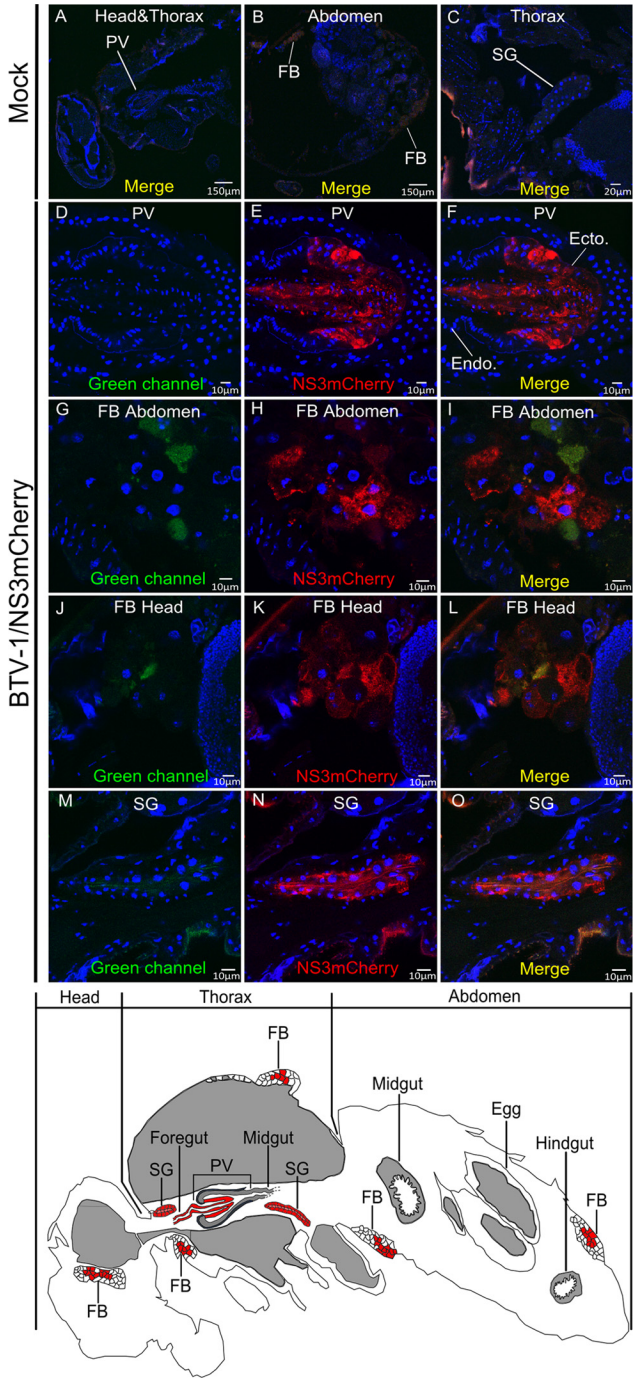

FIG 5 Confocal analysis of BTV-1/NS3mCherry tissue tropism. *D. melanogaster* (Yolk-T) flies were injected with BTV-1/NS3mCherry or virus-free medium (mock) and incubated for 10 days to allow viral replication. OCT-embedded flies were then sectioned and prepared for confocal analysis to assess BTV-1/NS3mCherry replication in tissues. (A to C) In all cases, the green channel is displayed to highlight tissue-derived background fluorescence. As expected, the mCherry signal was never detected in the head, thorax, or abdomen of mock-injected *D. melanogaster*. BTV-1/NS3mCherry efficiently replicated in the proventriculus (PV) (D to F), fat bodies (FB) of both the abdomen (G to I) and head (J to L), and the salivary glands (SG) (M to O) of infected *D. melanogaster* flies. (F) Note that in the PV, cells of ectodermal (Ecto) but not endodermal (Endo) origin were found positive for BTV-1/NS3mCherry replication. Scale bars, 10 μm. (Bottom) To illustrate the location of tissues/organs infected by BTV-1/NS3mCherry, a cartoon representing the sagittal section of *Drosophila* is shown.

gens, including members of the *Flaviviridae* (e.g., West Nile virus and dengue virus) (30, 76) and *Togaviridae* (e.g., chikungunya virus) (53) families. Our data show that BTV-1/NS3mCherry replicates efficiently only in tetracycline-treated *D. melanogaster* (which no longer contain detectable amounts of *W. pipientis*). Although this antibiotic treatment could potentially have other effects, our results suggest that the *W. pipientis*, in particular, a *w*Mel-related strain, is also able to inhibit BTV replication. Recent studies have demonstrated the use of the *w*Mel strain to control dengue fever in natural mosquito populations (37, 76). Future investigations will evaluate this approach to control animal pathogenic viruses transmitted by *Culicoides* vectors, such as BTV.

The natural route of BTV infection (via blood feeding) could not be applied in this study due to the different feeding behaviors of *Drosophila* (nonhematophagous) compared to *Culicoides* (hematophagous). The BTV-1/NS3mCherry virus was therefore injected directly into the insect hemocoel, bypassing any potential barriers to dissemination. In line with previously published data regarding BTV replication in *Culicoides* (26), we observed clear infection of fat bodies, salivary glands, and the foregut-midgut junction (proventriculus). BTV-1/NS3mCherry replication in the proventriculus was restricted to ectodermal cells (foregut origin), while the endodermal cells (midgut origin) were uninfected (27, 42). These data imply that BTV can enter from the basement membrane (e.g., membrane directly in contact with the hemocoel) of foregut cells but not midgut cells. Besides BTV, several other pathogenic arboviruses, including Venezuelan equine encephalitis virus and West Nile virus, have been shown to infect the foregut-midgut junction of their insect vectors (26, 29, 68). Therefore, infection of this organ may play a major role in the replication cycle of BTV in insects.

In summary, this study shows that reverse genetics can be used to generate BTVs expressing a viral protein tagged with a fluorescent molecule. We demonstrate that such a modified virus can replicate independently of helper cell lines and can be used for *in vivo* studies in an insect model. *D. melanogaster* offers a large array of well-developed molecular and genetic tools, which can be used to further investigate novel aspects of BTV-insect interactions that cannot be addressed in the natural vector species. In addition, BTV-1/NS3mCherry may also facilitate a better understanding of the role played by natural barriers in the modulation of species-specific susceptibility to BTV infection. Future experiments with orally infected midges using membrane-based blood-feeding techniques, which more closely resemble the natural route of infection, may reveal further details on BTV replication and dissemination within its insect vectors.

ACKNOWLEDGMENTS

This study was funded by the Ecole Pratique des Hautes Etudes, the Institut National de la Recherche Agronomique, the University of Lyon 1, the EMIDA program via the BBSRC, and Defra project SE2616 (United Kingdom).

We thank Alessia Armezzani and members of our laboratories for useful suggestions. We acknowledge the contribution of the biosafety level 3 (BSL3) and flow cytometry platforms of SFR BioSciences Gerland Lyon Sud (UMS3444/US8). We thank Barbara Gineys, Marie-Pierre Confort, Fabienne Archer, and Sebastien Dussurgey for their invaluable technical help and advice, Jean-Marc Reichhart for providing the *D. melanogaster* strain (w; P{w+, GAL4-YP1.JMR}20) employed in this study, and Eric Denison for the production of *Culicoides* used during the trials. Finally, we

thank Jean-Luc Imler and Carine Meignin for providing the *D. melanogaster* strain Canton-S.

REFERENCES

1. **Arnaud F, Murcia PR, Palmarini M.** 2007. Mechanisms of late restriction induced by an endogenous retrovirus. J. Virol. **81**:11441–11451.
2. **Bansal OB, Stokes A, Bansal A, Bishop D, Roy P.** 1998. Membrane organization of bluetongue virus nonstructural glycoprotein NS3. J. Virol. **72**:3362–3369.
3. **Baylis M, Mellor PS, Wittmann EJ, Rogers DJ.** 2001. Prediction of areas around the Mediterranean at risk of bluetongue by modelling the distribution of its vector using satellite imaging. Vet. Rec. **149**:639–643.
4. **Beaton AR, Rodriguez J, Reddy YK, Roy P.** 2002. The membrane trafficking protein calpactin forms a complex with bluetongue virus protein NS3 and mediates virus release. Proc. Natl. Acad. Sci. U. S. A. **99**: 13154–13159.
5. **Belhouchet M, et al.** 2011. Detection of a fourth orbivirus non-structural protein. PLoS One **6**:e25697. doi:10.1371/journal.pone.0025697.
6. **Blagrove MS, Arias-Goeta C, Failloux AB, Sinkins SP.** 2011. Wolbachia strain wMel induces cytoplasmic incompatibility and blocks dengue transmission in Aedes albopictus. Proc. Natl. Acad. Sci. U. S. A. [Epub ahead of print.] doi:10.1073/pnas.1112021108.
7. **Boorman J.** 1974. The maintenance of laboratory colonies of Culicoides variipennis (Coq.), C. nubeculosus (M.) and C. reithi (Keiff.). Bull. Entomol. Res. **64**:371–377.
8. **Boorman J.** 1986. Presence of bluetongue virus vectors on Rhodes. Vet. Rec. **118**:21.
9. **Bowne JG, Jones RH.** 1966. Observations on bluetongue virus in the salivary glands of an insect vector, Culicoides variipennis. Virology **30**: 127–133.
10. **Boyce M, Celma CC, Roy P.** 2008. Development of reverse genetics systems for bluetongue virus: recovery of infectious virus from synthetic RNA transcripts. J. Virol. **82**:8339–8348.
11. **Brookes SM, Hyatt AD, Eaton BT.** 1993. Characterization of virus inclusion bodies in bluetongue virus-infected cells. J. Gen. Virol. **74**(Pt 3): 525–530.
12. **Caporale M, et al.** 2011. Determinants of bluetongue virus virulence in murine models of disease. J. Virol. **85**:11479–11489.
13. **Caracappa S, et al.** 2003. Identification of a novel bluetongue virus vector species of Culicoides in Sicily. Vet. Rec. **153**:71–74.
14. **Carpenter S, Lunt HL, Arav D, Venter GJ, Mellor PS.** 2006. Oral susceptibility to bluetongue virus of Culicoides (Diptera: Ceratopogonidae) from the United Kingdom. J. Med. Entomol. **43**:73–78.
15. **Carpenter S, Wilson A, Mellor PS.** 2009. Culicoides and the emergence of bluetongue virus in northern Europe. Trends Microbiol. **17**:172–178.
16. **Celma CC, Roy P.** 2009. A viral nonstructural protein regulates bluetongue virus trafficking and release. J. Virol. **83**:6806–6816.
17. **Cherry S, Silverman N.** 2006. Host-pathogen interactions in drosophila: new tricks from an old friend. Nat. Immunol. **7**:911–917.
18. **Clark ME, Anderson CL, Cande J, Karr TL.** 2005. Widespread prevalence of wolbachia in laboratory stocks and the implications for Drosophila research. Genetics **170**:1667–1675.
19. **Darpel KE, et al.** 2007. Clinical signs and pathology shown by British sheep and cattle infected with bluetongue virus serotype 8 derived from the 2006 outbreak in northern Europe. Vet. Rec. **161**:253–261.
20. **De Liberato C, et al.** 2005. Identification of Culicoides obsoletus (Diptera: Ceratopogonidae) as a vector of bluetongue virus in central Italy. Vet. Rec. **156**:301–304.
21. **DuToit RM.** 1944. The transmission of blue-tongue and horse sickness by Culicoides. Onderstepoort J. Vet. Sci. Anim. Ind. **19**:7–16.
22. **Ferrandon D, Imler JL, Hetru C, Hoffmann JA.** 2007. The Drosophila systemic immune response: sensing and signalling during bacterial and fungal infections. Nat. Rev. Immunol. **7**:862–874.
23. **Finney DJ.** 1952. Statistical method in biological assay, p 524–531. Hafner Publishing Company, New York, NY.
24. **Foster NM, Jones RH.** 1979. Multiplication rate of bluetongue virus in the vector Culicoides variipennis (Diptera: Ceratopogonidae) infected orally. J. Med. Entomol. **15**:302–303.
25. **Fu H.** 1995. Mechanisms controlling the infection of Culicoides biting midges with bluetongue virus. Ph.D. thesis. University of Hertfordshire, Hertfordshire, United Kingdom.
26. **Fu H, Leake CJ, Mertens PP, Mellor PS.** 1999. The barriers to bluetongue virus infection, dissemination and transmission in the vector, Culicoides variipennis (Diptera: Ceratopogonidae). Arch. Virol. **144**:747–761.
27. **Fuss B, Josten F, Feix M, Hoch M.** 2004. Cell movements controlled by the Notch signalling cascade during foregut development in Drosophila. Development **131**:1587–1595.
28. **Georgel P, et al.** 2001. Drosophila immune deficiency (IMD) is a death domain protein that activates antibacterial defense and can promote apoptosis. Dev. Cell **1**:503–514.
29. **Girard YA, Klingler KA, Higgs S.** 2004. West Nile virus dissemination and tissue tropisms in orally infected Culex pipiens quinquefasciatus. Vector Borne Zoonotic Dis. **4**:109–122.
30. **Glaser RL, Meola MA.** 2010. The native Wolbachia endosymbionts of Drosophila melanogaster and Culex quinquefasciatus increase host resistance to West Nile virus infection. PLoS One **5**:e11977. doi:10.1371/journal.pone.0011977.
31. **Grimes JM, et al.** 1998. The atomic structure of the bluetongue virus core. Nature **395**:470–478.
32. **Grimes JM, et al.** 1997. An atomic model of the outer layer of the bluetongue virus core derived from X-ray crystallography and electron cryomicroscopy. Structure **5**:885–893.
33. **Gubbins S, Carpenter S, Baylis M, Wood JL, Mellor PS.** 2008. Assessing the risk of bluetongue to UK livestock: uncertainty and sensitivity analyses of a temperature-dependent model for the basic reproduction number. J. R. Soc. Interface **5**:363–371.
34. **Han Z, Harty RN.** 2004. The NS3 protein of bluetongue virus exhibits viroporin-like properties. J. Biol. Chem. **279**:43092–43097.
35. **Hanna SL, et al.** 2005. N-linked glycosylation of west nile virus envelope proteins influences particle assembly and infectivity. J. Virol. **79**:13262–13274.
36. **Hedges LM, Brownlie JC, O'Neill SL, Johnson KN.** 2008. Wolbachia and virus protection in insects. Science **322**:702.
37. **Hoffmann AA, et al.** 2011. Successful establishment of Wolbachia in Aedes populations to suppress dengue transmission. Nature **476**:454–457.
38. **Holden PR, Jones P, Brookfield JF.** 1993. Evidence for a Wolbachia symbiont in Drosophila melanogaster. Genet. Res. **62**:23–29.
39. **Hyatt AD, Zhao Y, Roy P.** 1993. Release of bluetongue virus-like particles from insect cells is mediated by BTV nonstructural protein NS3/NS3A. Virology **193**:592–603.
40. **Jennings DM, Mellor PS.** 1987. Variation in the responses of Culicoides variipennis (Diptera, Ceratopogonidae) to oral infection with bluetongue virus. Arch. Virol. **95**:177–182.
41. **Kim JM, et al.** 2008. A single N-linked glycosylation site in the Japanese encephalitis virus prM protein is critical for cell type-specific prM protein biogenesis, virus particle release, and pathogenicity in mice. J. Virol. **82**: 7846–7862.
42. **King DG.** 1988. Cellular organization and peritrophic membrane formation in the cardia (proventriculus) of Drosophila melanogaster. J. Morphol. **196**:253–282.
43. **Lemaitre B, Hoffmann J.** 2007. The host defense of Drosophila melanogaster. Annu. Rev. Immunol. **25**:697–743.
44. **Mellor PS, Carpenter S, Baylis M, Mertens PPC.** 2009. Bluetongue in Europe and the Mediterranean Basin, p 235–265. *In* Mellor PS, Baylis M, Mertens PPC (ed), Bluetongue monograph. Elsevier, Oxford, United Kingdom.
45. **Mellor PS.** 2004. Infection of the vectors and bluetongue epidemiology in Europe. Vet. Ital. **40**:167–174.
46. **Mellor PS.** 1990. The replication of bluetongue virus in Culicoides vectors. Curr. Top. Microbiol. Immunol. **162**:143–161.
47. **Mellor PS, Carpenter S, Harrup L, Baylis M, Mertens PP.** 2008. Bluetongue in Europe and the Mediterranean Basin: history of occurrence prior to 2006. Prev. Vet. Med. **87**:4–20.
48. **Mellor PS, Jennings M, Boorman JP.** 1984. Culicoides from Greece in relation to the spread of bluetongue virus. Rev. Elev. Med. Vet. Pays Trop. **37**:286–289.
49. **Mellor PS, Wittmann EJ.** 2002. Bluetongue virus in the Mediterranean Basin 1998–2001. Vet. J. **164**:20–37.
50. **Méroc E, et al.** 2009. Bluetongue in Belgium: episode II. Transbound Emerg. Dis. **56**:39–48.
51. **Mertens PP, Brown F, Sangar DV.** 1984. Assignment of the genome segments of bluetongue virus type 1 to the proteins which they encode. Virology **135**:207–217.
52. **Monastyrskaya K, Booth T, Nel L, Roy P.** 1994. Mutation of either of two

cysteine residues or deletion of the amino or carboxy terminus of nonstructural protein NS1 of bluetongue virus abrogates virus-specified tubule formation in insect cells. J. Virol. **68**:2169–2178.
53. **Mousson L, et al.** 2010. Wolbachia modulates Chikungunya replication in Aedes albopictus. Mol. Ecol. **19**:1953–1964.
54. **Murcia PR, Arnaud F, Palmarini M.** 2007. The transdominant endogenous retrovirus enJS56A1 associates with and blocks intracellular trafficking of Jaagsiekte sheep retrovirus Gag. J. Virol. **81**:1762–1772.
55. **Neil SJ, Eastman SW, Jouvenet N, Bieniasz PD.** 2006. HIV-1 Vpu promotes release and prevents endocytosis of nascent retrovirus particles from the plasma membrane. PLoS Pathog. **2**:e39. doi:10.1371/journal.ppat.0020039.
56. **O'Neill SL, Giordano R, Colbert AM, Karr TL, Robertson HM.** 1992. 16S rRNA phylogenetic analysis of the bacterial endosymbionts associated with cytoplasmic incompatibility in insects. Proc. Natl. Acad. Sci. U. S. A. **89**:2699–2702.
57. **Owens RJ, Limn C, Roy P.** 2004. Role of an arbovirus nonstructural protein in cellular pathogenesis and virus release. J. Virol. **78**:6649–6656.
58. **Papadopoulos O, Mellor PS, Mertens PPC.** 2009. Bluetongue control strategies. Bluetongue, p 429–452. *In* Mellor PS, Baylis M, Mertens PPC (ed), Bluetongue monograph. Elsevier, Oxford, United Kingdom.
59. **Purse BV, et al.** 2005. Climate change and the recent emergence of bluetongue in Europe. Nat. Rev. Microbiol. **3**:171–181.
60. **Ratinier M, et al.** 2011. Identification and characterization of a novel non-structural protein of bluetongue virus. PLoS Pathog. **7**:e1002477. doi:10.1371/journal.ppat.1002477.
61. **Roy P.** 2008. Bluetongue virus: dissection of the polymerase complex. J. Gen. Virol. **89**:1789–1804.
62. **Roy P.** 2008. Functional mapping of bluetongue virus proteins and their interactions with host proteins during virus replication. Cell Biochem. Biophys. **50**:143–157.
63. **Roy P, Marshall JJ, French TJ.** 1990. Structure of the bluetongue virus genome and its encoded proteins. Curr. Top. Microbiol. Immunol. **162**:43–87.
64. **Rubin GM.** 1988. Drosophila melanogaster as an experimental organism. Science **240**:1453–1459.
65. **Sabin LR, Hanna SL, Cherry S.** 2010. Innate antiviral immunity in Drosophila. Curr. Opin. Immunol. **22**:4–9.
66. **Savini G, et al.** 2005. Bluetongue virus isolations from midges belonging to the Obsoletus complex (Culicoides, Diptera: Ceratopogonidae) in Italy. Vet. Rec. **157**:133–139.
67. **Schwartz-Cornil I, et al.** 2008. Bluetongue virus: virology, pathogenesis and immunity. Vet. Res. **39**:46.
68. **Smith DR, Arrigo NC, Leal G, Muehlberger LE, Weaver SC.** 2007. Infection and dissemination of Venezuelan equine encephalitis virus in the epidemic mosquito vector, Aedes taeniorhynchus. Am. J. Trop. Med. Hyg. **77**:176–187.
69. **Teixeira L, Ferreira A, Ashburner M.** 2008. The bacterial symbiont Wolbachia induces resistance to RNA viral infections in Drosophila melanogaster. PLoS Biol. **6**:e1000002. doi:10.1371/journal.pbio.1000002.
70. **Thomas CP, Booth TF, Roy P.** 1990. Synthesis of bluetongue virus-encoded phosphoprotein and formation of inclusion bodies by recombinant baculovirus in insect cells: it binds the single-stranded RNA species. J. Gen. Virol. **71**(Pt 9):2073–2083.
71. **Toussaint JF, et al.** 2006. Bluetongue in northern Europe. Vet. Rec. **159**:327.
72. **Vallet-Gely I, Lemaitre B, Boccard F.** 2008. Bacterial strategies to overcome insect defences. Nat. Rev. Microbiol. **6**:302–313.
73. **Vassalos M.** 1980. Cas de fièvre catarrhale du mouton dans l'ile de Lesbos (Greece). Bull. Off. Int. Epizoot. **92**:547–555.
74. **Velthuis AG, Saatkamp HW, Mourits MC, de Koeijer AA, Elbers AR.** 2010. Financial consequences of the Dutch bluetongue serotype 8 epidemics of and 2007. Prev. Vet. Med. **93**:294–304.
75. **Veronesi E, et al.** 2008. Quantifying bluetongue virus in adult Culicoides biting midges (Diptera: Ceratopogonidae). J. Med. Entomol. **45**:129–132.
76. **Walker T, et al.** 2011. The wMel Wolbachia strain blocks dengue and invades caged Aedes aegypti populations. Nature **476**:450–453.
77. **Wechsler SJ, McHolland LE, Tabachnick WJ.** 1989. Cell lines from Culicoides variipennis (Diptera: Ceratopogonidae) support replication of bluetongue virus. J. Invertebr. Pathol. **54**:385–393.
78. **Wilson AJ, Mellor PS.** 2009. Bluetongue in Europe: past, present and future. Philos. Trans. R. Soc. Lond. B Biol. Sci. **364**:2669–2681.
79. **Wu X, Chen SY, Iwata H, Compans RW, Roy P.** 1992. Multiple glycoproteins synthesized by the smallest RNA segment (S10) of bluetongue virus. J. Virol. **66**:7104–7112.
80. **Zhou W, Rousset F, O'Neil S.** 1998. Phylogeny and PCR-based classification of Wolbachia strains using wsp gene sequences. Proc. Biol. Sci. **265**:509–515.